BEAM OPTICS SIMULATION STUDY ON THE PRE-STRIPPER LINAC FOR RARE ISOTOPE SCIENCE PROJECT*

J. W. Kim†, J. H. Jang, H. C. Jin, Institute for Basic Science, Daejeon, Korea
P. N. Ostroumov, B. Mustapha, J. A. Conway, Argonne National Laboratory, Argonne IL, USA

Abstract

The rare isotope science project (RISP) under development in Korea aims to provide various heavy-ion beams for nuclear and applied science users. A pre-stripper linac is the first superconducting section to be constructed for the acceleration of both stable and radioisotope beams to the energy of 18.5 Mev/u with a DC equivalent voltage of 160 MV. The current baseline design consists of an ECR ion source, an RFQ, cryomodules with QWR and HWR cavities and quadruple focusing magnets in the warm sections between cryomodules. Recently we have developed an alternative design in collaboration with Argonne's Linac Development Group to layout the linac based on state-of-the-art ANL's QWR operating at 81.25 MHz and multi-cavity cryomodules of the type used for the ATLAS upgrade and Fermilab PIP-II projects. End-to-end beam dynamics calculations have been performed to ensure an optimized design with no beam losses. The numbers of required cavities and cryomodules are significantly reduced in the alternative design. The results of beam optics simulations and error sensitivity studies are discussed.

INTRODUCTION

A next-generation rare isotope science facility using the in-flight fragment (IF) separation technique requires a high-current heavy-ion accelerator capable of delivering ^{238}U beam with a few hundred kW power to a thin production target [1]. First, high currents of highly charged ions are needed to efficiently produce such high-power heavy ion beams. An ECR ion source operating at 28 GHz [2] has been developed, but for the heaviest ions, the beam current in a single charge state is still lower than required for a next generation IF facility.

To fully utilize the available accelerating voltage of a heavy-ion linac, charge strippers are employed in the process of multi-step acceleration. To accelerate a uranium beam to 200 MeV/u, charge stripping at 18 MeV/u was determined to be optimal. A significant merit of a superconducting linac is that its longitudinal acceptance is large enough to simultaneously accelerate multiple charge states of uranium produced at the charge stripper. Therefore, a large fraction of the beam is accelerated after the stripper and beam losses in the charge state selection section are significantly reduced resulting in lower radiation levels in that region.

*Work supported by National Research Foundation Grant No. 20110018946 and the Rare Isotope Science Project.
†jwkim@ibs.re.kr

The layout of the pre-stripper linac of the Rare Isotope Science Project (RISP) ongoing in Korea [3] is shown in Fig 1. The linac is designed to accelerate either radioisotope beams from the ISOL target or stable beams from the ECR. In fact, a plan is to accelerate both radioisotope and stable beams simultaneously when their charge-to-mass ratios are within 2%. For instance, $^{132}Sn^{18+}$ can be accelerated together with $^{238}U^{33+}$. The isotope beam from ISOL is charge-bred before being injected into the pre-stripper linac. The charge breeding takes tens of ms in EBIS, which is under development at RISP [4], and stable ions can be accelerated during charge-breeding. Since the time duration for injection and extraction of isotope beams is much shorter than 1 ms and the breeding takes tens of ms, the fraction of stable beam can be over 90%. The simultaneous acceleration scheme of stable and radioisotope beams was devised for the proposed multi-user upgrade of the ATLAS linac at Argonne [5].

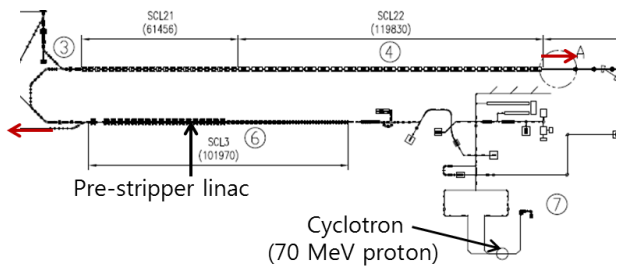

Figure 1: Layout of the pre-stripper linac of the RISP baseline design.

The injector includes an RFQ and the beam energy to the first cavity is 500 keV/u. The pulsing of stable ions according to the time structure of the charge-bred radioisotope beam is formed by an electric chopper. At the end of pre-stripper linac the two beams are switched by a kicker magnet either to low energy experimental area or to the achromatic 180° bending section after charge stripping.

CURRENT BEAM OPTICS DESIGN

The current design of the pre-stripper linac is based on the use of two kinds of superconducting cavities: QWR (β_{opt}=0.047) and HWR (β_{opt}=0.12) operating at 81.25 and 162.5 MHz, respectively [6]. Transverse focusing components were decided to be quadrupole doublets based on the thought that superconducting solenoids located inside cryomodule can affect the cavity

ISBN 978-3-95450-178-6

performance with leakage magnetic fields and also alignment of solenoids can be less accurate.

The numbers of sc-cavity and cryomodule of the current baseline design are listed in Table 1 in comparison with those of a new design proposal based on Argonne's cavities and cryomodules. In the baseline design, cryomodules of the first 22 units contain a single QWR cavity each, followed by cryomodules with two and four HWRs each. Both kinds of cavities are assumed to operate at a peak surface electric field (E_p) of 35 MV/m, while ANL's design assumes E_p to be 40 MV/m.

Table 1: Linac Parameters of the RISP Baseline Design in Comparison to the ANL Design Proposal

Parameters	RISP baseline	ANL proposal
Number of QWR (or QWR1)	22	15
Number of HWR (or QWR2)	102	49
Number of cryomodule	54	9
Total length	100 m	53.3 m

The main beam for the linac lattice design is ^{238}U, and TRACK [7] and TRACEWIN [8] have been used for the beam dynamics simulations. The beam phase spaces after RFQ acceleration were the input to the pre-stripper sc-linac. The RFQ is designed to have an adiabatic bunching section and a beam transmission higher than 98 %, which makes the longitudinal beam phase space at the end of the RFQ larger than for the design using an external multi-harmonic buncher (MHB).

The longitudinal acceptance of the linac and phase space of the U beam after the RFQ are shown in Fig. 2. They are carefully optimized for a proper matching and large margin, which requires slow ramping of acceleration voltages in the first few cavities and also for the cavities following the rf frequency jump from 81.25 MHz to 162.5 MHz.

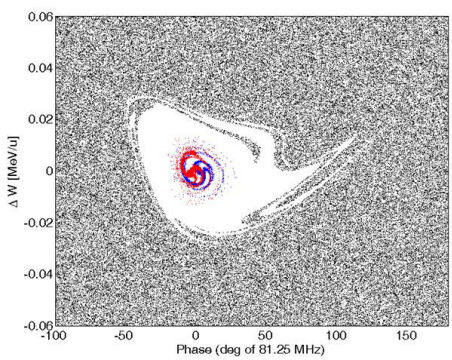

Figure 2: Longitudinal phase acceptance of the pre-stripper linac together with the phase space of a U beam.

A NEW DESIGN PROPOSAL

Considering the use of a large number of cavities and cryomodules in the current design and the risk in rf frequency jump in the middle of the linac, a new design using long cryomodules with superconducting solenoids based on realistic performance of ANL low-beta cavities has been proposed. This design study was performed in early 2016 utilizing two kinds of QWR cavities as mentioned in Table 1. Models of the QWR's with their electric field distributions are shown in Fig. 3 and their main parameters are listed in Table 2.

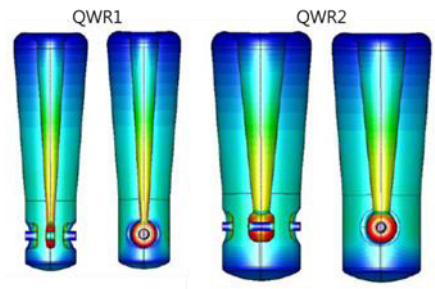

Figure 3: Electric field models of the two kinds of QWR's.

Table 2: Design Parameters of QWR1 and QWR2

Parameter	QWR1	QWR2
f (MHz)	81.25	81.25
β_{opt}	0.05	0.109
L_{eff} (cm)	18.5	40.2
E_{peak}/E_{acc}	5.6	5.6
B_{peak}/E_{acc} (mT/MeV/m)	7.7	7.3
R/Q (Ω)	493	552
G (Ω)	23	32
Aperture (mm)	40	40

The QWR cavities were designed to self-compensate the RF steering effects, therefore no active steering is needed in the linac when machine errors are not applied. The steering correction versus particle velocity for different tilt angles of the cavity's drift tube face was calculated. Figure 4 shows the beam steering in QWR1 for different steering correction angles including the uncorrected case (0°). It is clear that the 1° drift-tube face tilt is the closest to the zero line for the beam vertical angle (y'), which measures the steering effect. For QWR2 the beam steering effects can be similarly corrected with an angle of about 4°.

For the evaluation of the new linac lattice design, the goals of beam dynamics simulations were as follows: (1) to provide matching between the RFQ and the SC linac, (2) to define the value of the accelerating voltage and synchronous phase for each SC cavity and the solenoid field and (3) to demonstrate zero-loss beam acceleration in the pre-stripper linac.

ISBN 978-3-95450-178-6

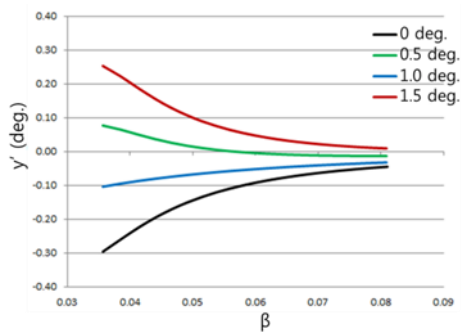

Figure 4: Steering correction for the QWR1. Vertical axis is the beam angle in the vertical plane which measures the steering due to the vertical asymmetry of the QWR geometry.

The simulation starts from a MHB with $U^{33+,34+}$. To define the parameters of the accelerating and focusing lattice, a relatively low number of particles is used, typically 10^4 for each charge state of uranium. The space charge effects for U beam are negligible after the RFQ, therefore we follow the dynamics of each charge state in the same accelerating bucket along the MEBT and pre-stripper linac. In realty each charge state occupies a separate bucket at the RFQ frequency.

The criteria for selection of the linac parameters is the proper matching in the transverse and longitudinal phase space for each focusing period along the linac. In particular, good matching must be provided in the transitions between cryomodules. Usually, a well-matched beam produces the lowest rms emittance growth. The available voltage from the SC resonators in the first two cryomodules exceeds the limit dictated by a smooth and adiabatic acceleration and can introduce significant non-linear motion in the longitudinal phase space if fully used. Therefore, we have applied ramping of both the accelerating voltage and synchronous phase in the first two cryomodules. Figure 5 shows a TRACK screenshot for the simulation of a U beam from the MHB to the end of the pre-stripper linac. The simulation starts with 5×10^5 particles in each charge state of 33+ and 34+, where 98.83 % particles are accepted by the RFQ and accelerated in the linac. It is important to note that there are no U beam losses along the SC linac.

To evaluate tolerances to misalignment and machine errors, beam simulations were performed for the linac including all sources of machine error. Three sets of errors with increasing amplitudes were simulated for $U^{33+,34+}$. Table 3 lists the error types and their values for every set of errors. It is important to note that for misalignment, the error given is the maximum absolute value used to generate a uniform error distribution, while for rf error, the sigma value is given for a Gaussian distribution truncated at 3σ. The Gaussian rf errors are to simulate jitter or dynamic errors that cannot be corrected for. Static rf errors are not included in these simulations because they are constant shifts in the cavity phase and amplitude that could, in principle, be measured and corrected.

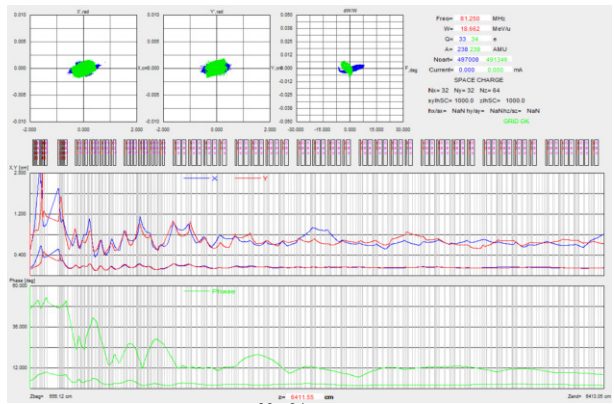

Figure 5: Evolution of $U^{33+,34+}$ beam envelopes (rms and full) along the MEBT and SC pre-stripper linac.

The first set of error in Table 3 represents the nominal error values and the rf errors were doubled in the second set, while the misalignment errors were doubled in the third one. For every error set, 100 randomly generated linac configurations (also known as seeds) were simulated, each with a total of 10^5 macro-particles starting from the LEBT ($5\text{x}10^5$ for each charge state). Both cases, before and after applying corrective steering, were simulated to study the effect of corrections and determine the required number, location and strengths of the steering coils.

Misalignment errors are uniformly generated within the given maximum values. RF errors are generated within a Gaussian truncated at the 3σ value given in table 3.

Table 3: Error Types and Amplitudes for Three Sets of Errors Used in the Simulations

Error set	Cavity & Solenoid misalignment (mm)	Cavity phase error (deg.)	Cavity amplitude error (%)
1	0.25	0.5	0.5
2	0.25	1.0	1.0
3	0.5	0.5	0.5

The transverse correction scheme used in the error simulations with corrective steering is shown in Fig. 6. In this scheme, every cryomodule is treated as a separate correction section. The general idea is to use the steering coils on the solenoids placed in the middle of the cryomodule and the beam position monitors attached to the solenoid placed at the cryomodule end and between cryomodules. For every correction section, at least two monitors are required in order to correct both the position and angle of the beam. Only two correctors and two monitors are used in this scheme. In the case where the combined strength of the two central correctors is not sufficient, a third corrector placed at the cryomodule entrance can be used. In these simulations, the corrector strength was limited to 5 mrad angular kick. The monitor precision and misalignment were set to 100 microns each. With increasing error amplitudes, the correction scheme

ISBN 978-3-95450-178-6

may fail at one point. In this case, we can include more correctors and monitors in every correction section and or increase the corrector strength.

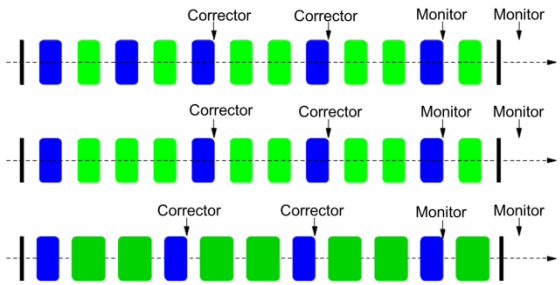

Figure 6: Correction scheme used in error simulations with corrective steering. The different strings correspond to the three different cryomodules of the linac, where every cryomodule is treated as a separate correction section.

The results of the error simulation with and without corrective steering are shown in Fig. 7 for the second error set. On the left, the figures show the beam centroids before (in red) and after correction (in blue). On the right, they show the distribution of angular kicks and the corresponding magnetic field strength required from the corrective steering coils. In comparison with the results of the other two error sets, we could see clearly that with increasing misalignment errors, the beam centroid spread after correction is wider and the required corrective field is stronger. It is important to note that the maximum required magnetic field integral for the corrective steering coils is 8000 G*cm, which would require a maximum magnetic field of 400 G for an effective coil length of 20 cm.

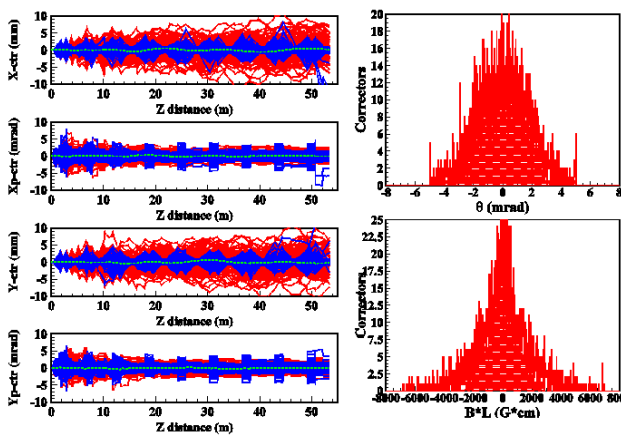

Figure 7: Error and correction simulation results for the second error set. On the left are beam centroids before and after correction. On the right are the corrector strength in mrad and the corresponding magnetic field integral in G*cm required.

The fractional beam losses before correction for the first two sets of errors were in the order of 5×10^{-7} and 5% for the third set. After correction, the loss becomes less than 1×10^{-7} for the second set, and almost zero for the other two sets. Based on the results of these error and correction simulations, we can conclude that the proposed design for the RISP pre-stripper linac is robust and offer a wide range of tolerance to errors and flexibility for beam tuning without any beam loss.

CRYOGENICS ASPECT

The operation temperature of the two kinds of QWR can be either 4.5 K or 2 K. It can be chosen considering the cryogenic budget depending on the operation temperature. In addition to the cryomodule thermal loads, heat loads on the cryogenic distribution system is included. The cryogenic distribution system for 2.0 K operation estimates is based upon supplying each cryomodule with 5 K helium gas where internal heat exchangers and J-T valves convert the 5 K supply to 2 K liquid/gas.

The result of cryogenic load estimation is summarized in Table 4. It is worthwhile to point out that the total required operating power at 2.0 K is double that for 4.4 K operation. This is because the static heat leak is large relative to the dynamic loads. Even though the dynamic thermal load decreases by almost a factor of 5 from 781 W at 4.4 K to 198 W at 2.0 K, the static loads do not follow the same trend.

The new design assumes to operate the two kinds of QWR at 4.5 K. The capacity of cryogenic plant considered is 2.5 kW at 4.4 K while it is 4.2 kW for the pre-stripper linac of the current baseline design.

Table 4: Cryogenic Heat Loads for 2.0 K and 4.4 K Operation for the ANL Design Study

T_{op}	Cryomodules	Distribution	Total at 4.4 K
2.0 K	435 W	355 W	2.64 kW
4.4 K	985 W	355 W	1.34 kW

SUMMARY

A new design of pre-stripper linac has been studied in comparison with the present baseline design of RISP. The new design uses much less number of cavities and cryomodules by adopting state-of the art cavities in operation at ANL [9, 10]. The lattice design includes 5.7 m long cryomodules and superconducting solenoid focusing magnets. Beam optics study including error analysis shows similar tolerances with that of present baseline design. A significant saving in cryogenic system and long-term operation costs is also expected.

REFERENCES

[1] J. A. Nolen, Nucl. Phys. A 787, 84 (2007).
[2] G. Machicoane et al., "Design Status of ECR ion source and LEBT for FRIB", Proc. of ECRIS 2012, Sydney, Australia (2012), p.172.

ISBN 978-3-95450-178-6

[3] S.C. Jeong, "Progress of the RAON heavy ion accelerator project in Korea", Proc. of IPAC 2016 Conf., Busan, Korea May, 2016, p.4261.
[4] S. Kondrashev, J. Kim, Y. Park, H. Son, Advanced EBIS charge breeder for Rare Isotope Science Project, Proc. of IPAC 2016 Conf., Busan, Korea May, 2016, p.1304.
[5] B. Mustapha et al, "Simultaneous acceleration of radioactive and stable Beams in the ATLAS Linac" Proc. of HB2014, East Lansing, Michigan, 2014, p334.
[6] D. Jeon et al, J. Korean Phys. Soc. 65, 1010 (2014).
[7] P.N. Ostroumov, V. Aseev and B. Mustapha, TRACK, ANL Technical Note, Updated for version 3.7.
[8] D. Uriot and N. Pichoff, "TraceWin", CEA Saclay, June 2014.
[9] P.N. Ostroumov et al., "Completion of efficiency and intensity upgrade of the ATLAS facility", Proc. of LINAC2014, Geneva, Switzerland, 2014, p.449.
[10] M.P. Kelly et al., "Commissioning of the 72 MHz quarter-wave cavity cryomodule at ATLAS", Proc. of LINAC2014, Geneva, Switzerland, 2014, p.440.

ISBN 978-3-95450-178-6